Journal of Hazardous Materials 256–257 (2013) 1–9

Contents lists available at SciVerse ScienceDirect

Journal of Hazardous Materials

journal homepage: www.elsevier.com/locate/jhazmat

Heterogeneity of biochar properties as a function of feedstock sources and production temperatures

Ling Zhao [a], Xinde Cao [a,*], Ondřej Mašek [b], Andrew Zimmerman [c]

[a] School of Environmental Science and Engineering, Shanghai Jiao Tong University, Shanghai 200240, China
[b] School of Geosciences, University of Edinburgh, Kings Buildings, Edinburgh EH9 3JN, UK
[c] Department of Geological Sciences, University of Florida, Gainesville, FL 32611, USA

HIGHLIGHTS

- Feedstock and temperature influence specific biochar properties to a different extent.
- Heterogeneity depended on feedstock and temperature were compared quantitatively.
- Carbon sequestration, fixed C and minerals were determined by feedstock.
- Biochar pH, specific surface area and recalcitrance were dominated by temperature.
- Alkyl-C, aliphatic-C and aromatic-C were more highly related to temperature.

ARTICLE INFO

Article history:
Received 28 December 2012
Received in revised form 28 March 2013
Accepted 10 April 2013
Available online 17 April 2013

Keywords:
Biochar
Feedstock-depended heterogeneity
Temperature-depended heterogeneity
Physiochemical properties
Chemical structure

ABSTRACT

The aim of this study was to quantify the influence of the two main categories of factors determining the yield and properties of biochar, i.e., feedstock properties and production conditions, here represented by the highest treatment temperature (HTT). To achieve this, a wide range of production temperatures (200–650 °C) and an extensive set of diverse feedstock ($n = 12$) were used to calculate the sensitivity. The quantitative evaluation was based on statistical analysis of coefficients of variation, and thus derived indices representing the extent of influence of the two factors, i.e., a feedstock-depended heterogeneity (H_F) and a temperature-depended heterogeneity (H_T). The results showed that both feedstock properties and production conditions are important for determining the yield and properties of biochar, but their respective influence changes with the property or set of properties of interest. The biochar parameters most affected by feedstock properties were e.g., total organic carbon, fixed carbon, and mineral elements of biochar. On the other hand, biochar surface area and pH was mainly influenced by highest treatment temperature. Biochar recalcitrance was mainly determined by production temperature, while the potential total C sequestration (product of recalcitrance and pyrolysis carbon yield) depended more on feedstock. Overall, the work sheds some light on the relative importance of different biochar production process parameters on the final biochar product, which is an important step towards "designed" biochar.

1. Introduction

Biochar, a carbonaceous solid product of pyrolysis (thermochemical decomposition in absence of oxygen) of organic materials, such as biomass, has progressively been receiving increased attention. This is due to several factors: first, it is one of very few technologies that can actively remove carbon from the atmosphere [1–3]; second, it is suitable for a range of environmental applications, in particular low quality soils [4–6]; third, it offers the potential to improve the productivity of soils (while still offering at least some of the other benefits) [7,8]. However, the utility of a specific biochar for any particular application depends on its inherent properties. For example, biochar with high specific surface area may be used as sorbents, whereas the ones with high recalcitrance may function in carbon fixation [9]. Those rich in available nutrients and minerals and/or showing high water holding capacity could be better used as soil amendments to improve fertility [10].

It has been shown that biochar characteristics are influenced by production variables such as feedstock, highest treatment temperature, holding time at HTT, pyrolysis atmosphere, etc. Among these, feedstock properties (both physical and chemical) and HTT are considered to be among the main factors influencing

* Corresponding author. Tel.: +86 21 54743926; fax: +86 21 54740825.
E-mail addresses: xdcao@sjtu.edu.cn, xindecao@yahoo.com (X. Cao).

0304-3894/$ – see front matter © 2013 Elsevier B.V. All rights reserved.
http://dx.doi.org/10.1016/j.jhazmat.2013.04.015

biochar characteristics [11–13]. For example, increases of pH, CEC, and trace metals concentration occur with increasing production temperature [14–16]. Biochars derived from wood biomasses often have higher surface area than grass biochar [16,17]. However, most previous studies focused on the impact of production parameters on physic-chemical properties of biochar used either a narrow range of feedstock materials, often falling into one or two categories such as agricultural residues, wood derivatives, or manures, or a narrow range of production temperatures. For example, Cantrell et al. [18] studied the impact of pyrolysis temperature and manure source on physicochemical characteristics of five manures biochar made at only two temperatures. Pereira et al. [19] investigated the labile fraction of C in biochar derived from three trees (pine, poplar and willow) at two temperatures. Biochars of the feedstock with the same category might show similar properties compared to those made from parent material of very different types.

If the benefits offered by biochar are to be maximized, it is important to develop an understanding of its physiochemical variations and their relations to functions in soil for a broad range of biochar types. Optimizing biochar for a specific application may require a purposeful selection of a feedstock as well as pyrolysis production technique process, within constraints given by particular scenario, to produce biochar with desired characteristics [20]. Thus, the objectives of this study are (i) to determine how the two main factors, feedstock and HTT, affect selected biochar properties and (ii) to evaluate the relative importance of these factors on selected biochar properties/sets of properties related to its function in soil amendment and carbon storage. Two indices, H_F (feedstock-dependent heterogeneity) and H_T (temperature-dependent heterogeneity), based on statistical analysis of coefficient of variation, are introduced to quantify the influence of feedstock and HTT, respectively, on a selected set of any given biochar properties and identify which is dominant. This provides an insight and guidance necessary for informed selection of starting material and pyrolysis temperature for production of biochar with specified properties.

2. Materials and methods

2.1. Biomass collection and biochar production

Twelve common organic residues were collected from a farm in Shanghai, China and divided into 6 categories spanning animal manures, waste wood, crop residues, food waste, aquatic plants, and municipal waste. The biomass was air-dried (60 °C) to being with the moisture lower than 5% and then ground to less than 2 mm for biochar production. Details on the production of biochar were described previously [21]. Briefly, to evaluate the feedstock effects, all 12 dried and ground feedstock were heated to 500 °C under N_2 atmosphere with a heating rate of 18 °C min^{-1} and hold for 4 h. The long holding time at the HTT was selected to minimize effects of pyrolysis kinetics that could result in incomplete conversion especially during pyrolysis at low temperatures and thus affect observed results. To examine pyrolysis temperature effect, a wastes-based feedstock (pig manure) and plant-based feedstock (wheat straw) were chosen and pyrolyzed at HTT of 200 °C, 350 °C, 500 °C and 650 °C, with the same holding time at HTT (4 h).

2.2. Biochar characterization

Total C analysis of biochar was conducted on an element analyzer (Vario EL III, Elementar, Germany). Ash content, volatile matters (VM), and fixed carbon (FC) were determined according to standard ASTM methods [22–24]. The metal concentrations in biochar were measured in the digestion solution using the inductively coupled plasma (ICP-AES, ICAP6000 Radial, Thermo, English), following biochar digestion using the USEPA method 3050B [25]. The cation exchange capacity (CEC) was determined according to a modified barium chloride compulsive exchange method [26]. pH of biochar was measured using the 24 hour-equilibrated solution of biochar and deionized water with a solid/liquid ratio of 1:20 (w/v). All analyses were conducted in duplicate.

The solid phase of biochar was characterized by thermogravimetric analyser (TGA) (PerkinElmer Pyris 1 TGA) with heating from 25 °C to 900 °C under air atmosphere at a rate of 20 °C per min. Surface functional group distributions were determined by FTIR spectroscopy (IR Prestige 21 FTIR, Shimadzu, Japan) and nuclear magnetic resonance spectra (CP-MAS ^{13}C-NMR), which were obtained at a frequency of 100.6 MHz using a Varian Unity Inova 400 NMR spectrometer (AVANCE III 400, Bruker, Switzerland). Specific surface area and pore size distribution of biochars were determined using a BET-N_2 SA analyzer (JW-BK222, Jwgb, China). Raman spectroscopy analysis was conducted using a visible Raman system (Bruker Senterra R200-L, American) with a 15 mW 532 nm He–Ne laser with excitation line set to λ_0 = 532 nm.

2.3. Calculations

Fixed Carbon (FC) of biochar was calculated as the sum of moisture, ash, and volatile matter subtracted from 100 [24].

$$\mathrm{FC}(\%) = 100 - \mathrm{moisture}(\%) - \mathrm{ash}(\%) - \mathrm{VM}(\%) \quad (1)$$

An index R_{50} was used to evaluate the thermal recalcitrance of biochar and was obtained by TG analysis, as recently proposed by Harvey et al. [27]:

$$R_{50,\,\mathrm{biochar}} = \frac{T_{50,\,\mathrm{biochar}}}{T_{50,\,\mathrm{graphite}}} \quad (2)$$

where $T_{50,\,\mathrm{biochar}}$ and $T_{50,\,\mathrm{graphite}}$ are the temperature values corresponding to 50% weight loss by oxidation/volatilization of biochar and graphite, respectively, in air. Values are obtained directly from TG thermograms that have been corrected for water and ash content.

Carbon sequestration potential (CS) was defined as the final carbon that would be retained in soil. This was calculated by subtracting the carbon lost during pyrolysis from the initial C in raw biomass, and multiplying by the recalcitrance (R_{50}) of C in the biochar product. M was the weight of the feedstock.

$$\mathrm{CS}(\%) = \frac{M(\mathrm{g}) \cdot \mathrm{yield}(\%) \cdot C\%\,\mathrm{biochar} \cdot R_{50}}{M(\mathrm{g}) \cdot C\%\,\mathrm{feedstock}} \quad (3)$$

The feedstock-depended heterogeneity (H_F) and temperature-depended heterogeneity (H_T) of biochars were calculated using the coefficient of variation (CV) in statistical method, and the larger the H_F or H_T is, the more influenced by feedstock or production temperature the biochar property is:

$$H_F \quad \text{or} \quad H_T = \frac{\text{standard deviation}}{\text{mean value}} \quad (4)$$

3. Results and discussion

3.1. Bulk physicochemical properties

The results of analysis of bulk physicochemical properties of all 20 biochars produced are shown in Table 1. From the data, it can be seen that the content of total carbon (TC) shows relatively low variance, as a function of temperature for both feedstock tested, i.e., pig manure biochar (H_T = 0.09) and wheat straw biochar (H_T = 0.23), and only moderately dependent on feedstock (H_F = 0.37). On the other hand, the content of fixed carbon (FC), which has been also

Table 1
Compositions, physico-chemical properties, and structural characteristics of biochars derived from 12 waste biomasses produced at 500 °C and biochars produced from pig manure and wheat straw at 200–650 °C (dry basis).

Biochar feedstock	Temperature[a]	TC (%)[b]	FC (%)[c]	CS (%)[d]	Yield (%)	VM (%)[e]	Ash (%)	pH	CEC (cmol kg^{-1})[f]	SA (m^2 g^{-1})[g]	PV (cm^3 g^{-1})[h]	APS (nm)[i]	R_{50}[j]	I_D/I_G[k]
Cow manure	500 °C	43.7	14.7	41.8	57.2	17.2	67.5	10.2	149	21.9	0.028	5.04	0.57	1.09
Pig manure		42.7	40.2	26.6	38.5	11.0	48.4	10.5	82.8	47.4	0.075	6.35	0.59	1.19
Shrimp hull		52.1	18.9	34.3	33.4	26.6	53.8	10.3	389	13.3	0.039	11.6	0.83	1.51
Bone dregs		24.2	10.5	23.0	48.7	11.0	77.6	9.57	87.9	113	0.278	9.86	0.67	1.15
Wastewater sludge		26.6	20.6	21.1	45.9	15.8	61.9	8.82	168	71.6	0.060	3.37	0.68	–
Waste paper		56.0	16.4	24.7	36.6	30.0	53.5	9.88	516	133	0.084	2.51	0.70	1.29
Sawdust		75.8	72.0	28.5	28.3	17.5	9.94	10.5	41.7	203	0.125	2.23	0.67	1.33
Grass		62.1	59.2	28.0	27.8	18.9	20.8	10.2	84.0	3.33	0.010	11.9	0.71	1.20
Wheat straw		62.9	63.7	26.4	29.8	17.6	18.0	10.2	95.5	33.2	0.051	6.10	0.54	1.10
Peanut shell		73.7	72.9	34.4	32.0	16.0	10.6	10.5	44.5	43.5	0.040	3.72	0.61	1.15
Chlorella		39.3	17.4	33.0	40.2	29.3	52.6	10.8	562	2.78	0.010	15.0	0.72	1.16
Waterweeds		25.6	3.84	47.1	58.4	32.4	63.5	10.3	509	3.78	0.009	9.52	0.68	0.80
	H_F[l]	0.37	0.76	0.25	0.27	0.36	0.53	0.05	0.90	1.09	1.11	0.58	0.11	0.31
Pig manure	200 °C	37.0	12.6	45.1	98.0	50.7	35.7	8.22	23.6	3.59	–	–	0.46	–
	350 °C	39.1	34.7	31.5	57.5	27.4	37.2	9.65	49.0	4.26	0.024	12.8	0.52	0.56
	500 °C	42.7	40.2	26.6	38.5	11.0	48.4	10.5	82.8	47.4	0.075	6.35	0.59	1.19
	650 °C	45.3	19.2	31.4	35.8	10.7	69.6	10.8	132	42.4	0.062	5.80	0.71	0.90
	H_T[m]	0.09	0.48	0.24	0.50	0.76	0.33	0.12	0.65	0.97	0.49	0.47	0.19	0.36
Wheat straw	200 °C	38.7	22.5	40.7	99.3	70.2	7.21	5.43	32.1	2.53	–	–	0.41	–
	350 °C	59.8	53.2	45.3	52.5	31.3	14.7	8.69	87.2	3.48	0.010	11.3	0.56	1.24
	500 °C	62.9	63.7	26.3	29.8	17.6	18.0	10.2	95.5	33.2	0.051	6.10	0.54	1.16
	650 °C	68.9	72.1	34.1	26.8	11.1	16.2	10.2	146	182	0.093	2.05	0.71	1.32
	H_T	0.23	0.41	0.23	0.64	0.81	0.34	0.26	0.52	1.55	0.808	0.72	0.22	0.06

[a] Biochar production temperature.
[b] Total carbon.
[c] FC is fixed carbon (%, dry basis).
[d] CS is potential carbon sequestration (%) after pyrolysis and mineralization.
[e] VM is volatile matter (%, dry basis).
[f] CEC is cation exchange capacity (cmol kg^{-1}).
[g] SA is BET-N_2 surface area (m^2 g^{-1}).
[h] PV is pore volume (cm^3 g^{-1}).
[i] APS is average pore diameter (nm).
[j] R_{50} is a novel index for evaluating biochar recalcitrance derived from thermogravimetric data (Harvey et al. [27]).
[k] I_D/I_G, ratio of D-band and G-band from Raman spectra.
[l] H_F, feedstock-dependant heterogeneity index (see text).
[m] H_T, temperature-dependant heterogeneity index (see text).

Table 2
Mineral constituents (g kg^{-1}) of biochars derived from 12 waste biomasses produced at 500 °C and biochars produced from pig manure and wheat straw at 200–650 °C.

Biochar feedstock	Temperature[a]	P	K	Ca	Mg	Cu	Zn	Al	Fe	Mn
Cow manure	500 °C	0.646	1.021	3.795	1.569	0.013	0.052	0.506	0.616	0.044
Pig manure		4.386	3.560	3.474	2.801	0.078	0.101	0.455	0.696	0.123
Shrimp hull		2.585	1.896	21.03	0.590	0.013	0.015	0.024	0.023	0.006
Bone dregs		10.86	0.444	31.82	0.508	0.001	0.016	0.010	0.009	0.001
Wastewater sludge		1.702	0.525	6.573	0.645	0.038	0.152	1.929	2.209	0.045
Waste paper		0.124	0.079	22.84	0.584	0.001	0.010	0.361	0.455	0.008
Sawdust		0.061	1.189	2.290	0.348	0.001	0.010	0.097	0.168	0.009
Grass		0.590	5.151	5.236	0.530	0.003	0.023	0.109	0.152	0.011
Wheat straw		0.074	5.182	0.954	0.297	0.001	0.002	0.047	0.074	0.007
Peanut shell		0.166	1.733	1.338	0.458	0.002	0.003	0.218	0.256	0.018
Chlorella		0.717	13.67	17.50	0.779	0.003	0.012	0.547	0.409	0.912
Waterweeds		0.514	3.224	23.13	0.663	0.002	0.010	0.685	0.559	1.025
	H_F[b]	1.66	1.19	0.93	0.87	1.78	1.37	1.27	1.27	2.00
Pig manure	200 °C	1.72	1.40	1.36	1.10	0.031	0.040	0.179	0.273	0.048
	350 °C	2.94	2.38	2.33	1.88	0.052	0.068	0.305	0.466	0.082
	500 °C	4.39	3.56	3.47	2.80	0.078	0.101	0.455	0.696	0.123
	650 °C	4.72	3.83	3.74	3.02	0.084	0.109	0.490	0.749	0.132
	H_T[c]	0.40	0.40	0.40	0.40	0.40	0.40	0.40	0.40	0.40
Wheat straw	200 °C	0.022	1.55	0.286	0.089	0.000	0.001	0.014	0.022	0.002
	350 °C	0.042	2.94	0.540	0.168	0.001	0.001	0.027	0.042	0.004
	500 °C	0.074	5.18	0.95	0.297	0.001	0.002	0.047	0.074	0.007
	650 °C	0.082	5.75	1.06	0.329	0.001	0.002	0.052	0.082	0.008
	H_T	0.51	0.51	0.51	0.51	0.51	0.51	0.51	0.51	0.51

[a] Biochar production temperature.
[b] H_F, feedstock-depended heterogeneity (see text).
[c] H_T, temperature-depended heterogeneity (see text).

proposed as a potential measure for estimating biochar recalcitrance [13,28], has shown to be moderately dependent on HTT, i.e., pig manure biochar (H_T = 0.48) and wheat straw biochar (H_T = 0.41), and relatively strongly dependent on feedstock (H_F = 0.76). As all the H_T were considerably lower than the corresponding H_F values, it can be concluded that TC and FC of biochars were influenced more by feedstock choice than by HTT in the production process. Both volatile matter (VM) and weight yield were more sensitive to temperature indicated by their higher H_T (0.5–0.81) than H_F (0.27–0.36). Ash content was more sensitive to feedstock as indicated by its higher H_F (0.53) compared to H_T (0.33–0.34). As shown in Table 1, some of the biochar used in this study had very high ash content, e.g., manure and sludge biochar (18.1–42.9%), while crop residue biochar showed relatively low ash content (2.10–7.49%). The high ash content in the manure biochar was due to high concentration of mineral constituents in the feedstock [21]. Similarly to the ash content, the content of individual minerals showed very strong dependence on feedstock (H_F = 0.87–2.00) and only moderate dependence on HTT (H_T = 0.40–0.51), indicating that mineral elements of biochars were more influenced by feedstock composition than by pyrolysis temperature. Generally, manure biochar contained more P (plant nutrient) than crop residue and grass biochar [29]. On the other hand, crop residue and grass biochar contained more K than manure biochar (Table 2). Thus, this data suggest that the selection of biochar for soil amendment, aimed at improvement of soil fertility by addition of nutrients, should preferentially focus on feedstock selection rather than production temperature (although HTT can affect the availability of nutrients in biochar) [30].

Biochar pH varied less among the different feedstocks (8.8–10.8) than among the production temperature (5.43–10.8) (Table 1). Therefore, biochar was influenced more by temperature (H_T = 0.19) than by feedstock (H_F = 0.05). By contrast, the cation exchange capacity (CEC) varied greatly among biochar produced from different of different feedstock (H_F = 0.9) and only moderately with temperature (H_F = 0.52–0.65). This may be explained by the fact that CEC is related to cations (e.g., K, Ca, Mg) present in biochar, which vary greatly with feedstock (Table 2).

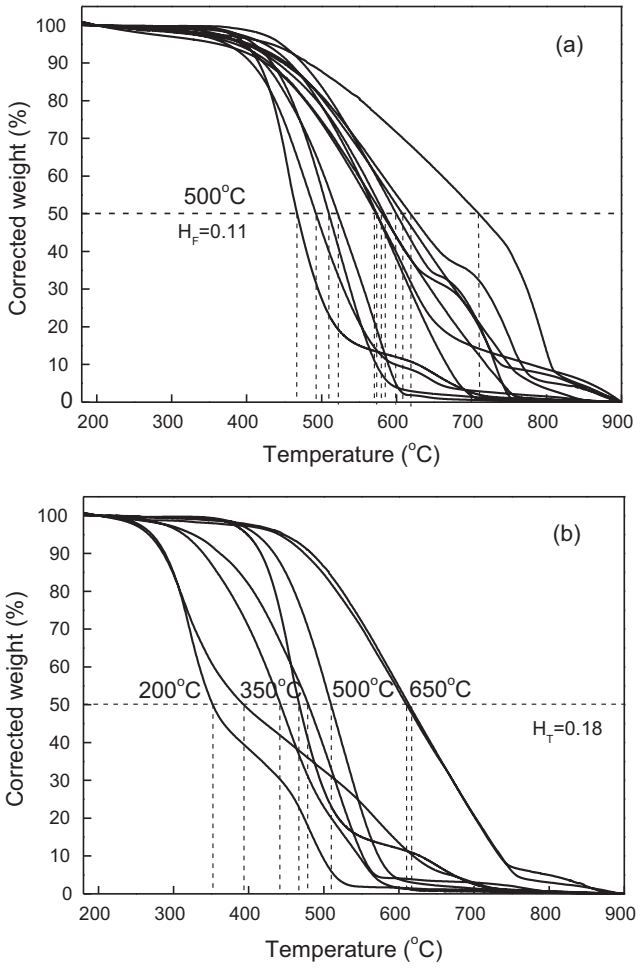

Fig. 1. Corrected thermogravimetry patterns of biochars derived from 12 feedstocks at 500 °C (a) and biochar produced from pig manure and wheat straw at 200–650 °C (b).

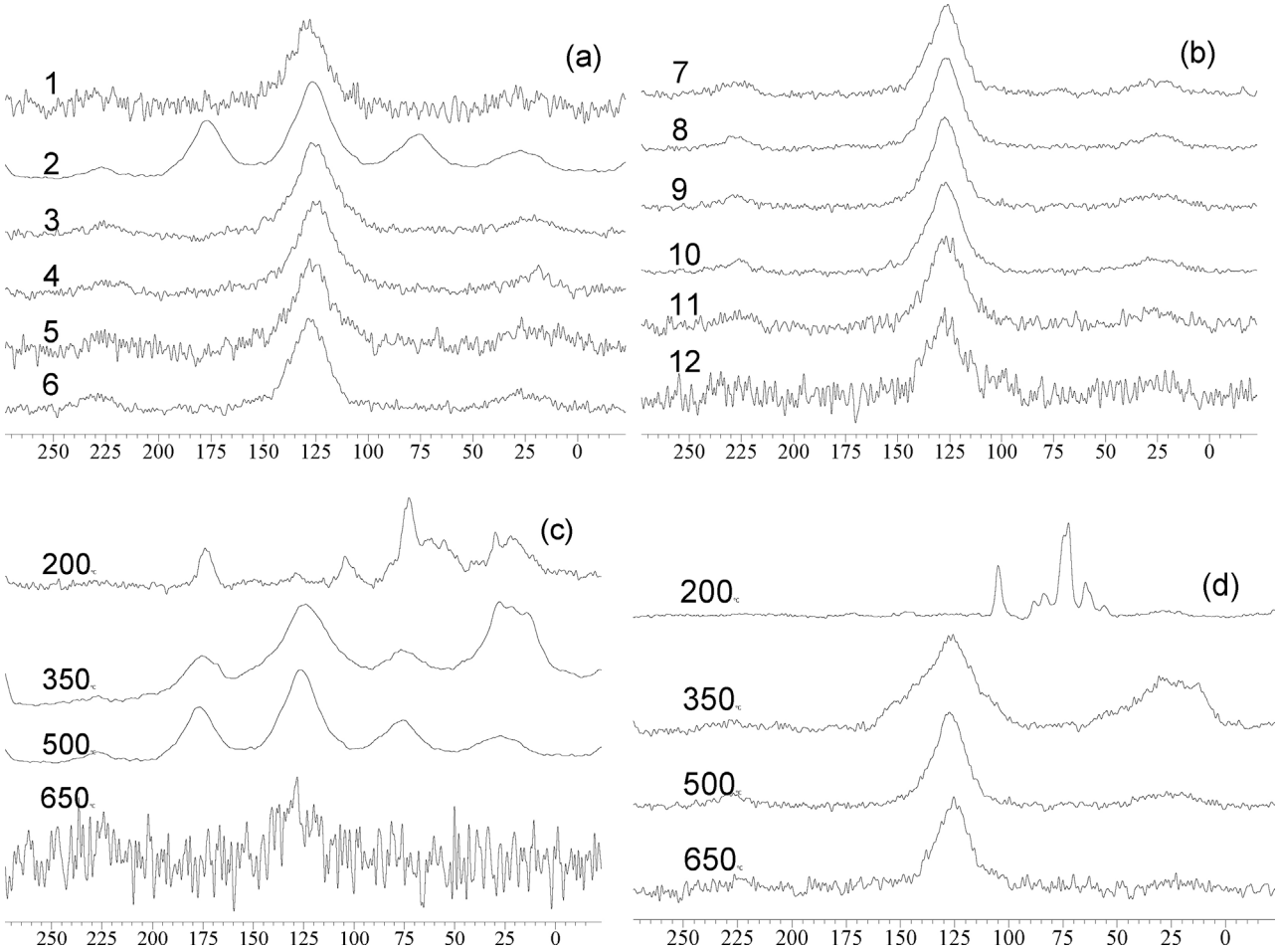

Fig. 2. CP-MAS ^{13}C NMR spectrogram of biochars derived from 12 feedstocks at 500 °C (a and b) and biochar produced from pig manure (c), and wheat straw at 200–650 °C (d). (1) Cow manure; (2) pig manure; (3) shrimp hull; (4) bone dregs; (5) wastewater sludge; (6) waste paper; (7) sawdust; (8) grass; (9) wheat straw; (10) peanut shell; (11) chlorella and (12) waterweeds.

The physical structure of biochars, such as surface area (SA), pore volume (PV), and average pore size (APS) are typically related to its sorption and water holding capacity which, in turn, relates to its effect on soil structure, contaminant mobility, and microbial interactions. The heterogeneities of SA and APS showed medium to very strong dependence on both the production temperature (H_T = 0.72–1.55) and feedstock (H_F = 0.58–1.09). Similar result was obtained for PV. The influence of feedstock on PV was perhaps related to the relative proportion of hemicelluloses, cellulose, and lignin fractions in biomasses. A dramatic rise in SA was observed when the temperature was increased above 350 °C, at which point, cellulose is known to decompose and a phase transition from layered C to amorphous char occurs [31].

3.2. Recalcitrance and stability

The ability of biochar to resist abiotic and biotic degradation (herein referred to as recalcitrance) is crucial to their function of sequestration of atmospheric carbon in soil. Harvey et al. [37] have developed an index (R_{50}) to evaluate the recalcitrance of biochars, which uses the energy required for thermal oxidation of biochar (normalized to that for oxidation of graphite) as a measure of recalcitrance [27].

The water and ash content-corrected thermogravimetry patterns of biochar are presented in Fig. 1. The temperatures at which 50% biochar weight loss occurred ranged between 467–710 °C for all feedstocks and within 352–613 °C for all production temperature of pig manure biochar and wheat straw biochar. The calculated R_{50} for biochars from all feedstocks fell in a range of 0.54–0.83, with H_F being 0.11, while R_{50} for biochars produced at 200–650 °C was within a wider range of 0.41–0.71, with H_T being 0.21 (Table 1), indicating that the recalcitrance of biochar was mainly determined by HTT (at least when holding time is sufficiently long), which confirms previous findings [9,28]. Biochar recalcitrance is among others, related to aromatic C which increased with increasing temperature, and the loss of N driven off by higher HTT [32]. Fig. 1 also shows that all biochars produced at same temperature had similar R_{50}, further suggesting that temperature was the dominating control on recalcitrance.

Carbon sequestration potential (CS) was evaluated using the R_{50} index as shown in Eq. (3). CS of all 12 biochars ranged 21.1–47.1% with H_F being 0.25, while those for pig manure biochar and wheat straw biochar at production temperature of 200–650 °C were 26.6–45.1% and 26.3–45.3%, respectively, with H_T being 0.24 and 0.23, respectively. The H_T and H_F are similar and all low, indicating that temperature and feedstock all had less influence on the carbon sequestration capacity. This is due to the fact that although lower temperature yield more char, its recalcitrance is low, i.e., a considerable amount of biochar C would be abiotically or microbially mineralized [9,33]; on the other hand, high pyrolysis temperatures yield less biochar, but its recalcitrance is high [34]. The C sequestration capacity

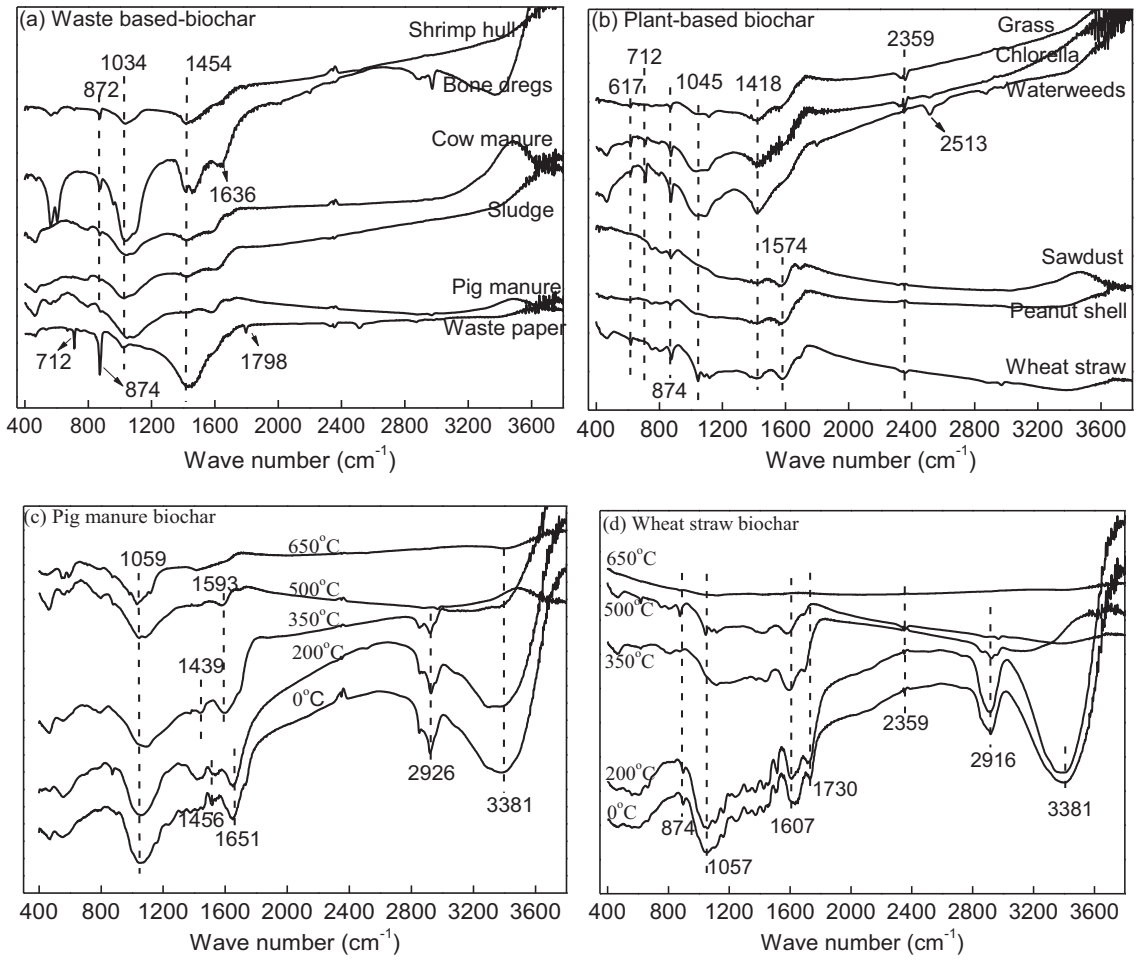

Fig. 3. FTIR spectra of biochars derived from 12 feedstocks at 500 °C (a and b) and biochars produced from pig manure (c) and wheat straw at production temperature ranging 200–650 °C (d).

was mainly determined by the inherent molecular configuration of biomass feedstock, which is perhaps of not much variety [35].

3.3. Biochar chemical structure

The carbon cluster size and functional group distributions were identified by CP-MAS ^{13}C NMR and FTIR, and are shown in Figs. 2 and 3, respectively. The ^{13}C NMR spectrograms of biochars from 12 feedstocks were very similar, whereas they varied greatly among those produced from a single feedstock type across a range of temperatures (Fig. 2). Table 3 summarizes the relative proportion of C in each chemical functional groups for the biochars examined, which were integrated in the chemical shift (ppm) resonance intervals of 0–46, 46–65, 65–90, 90–108, 108–145, 145–160, 160–185, 185–225 ppm [36]. Clearly, aromatic C with chemical shift of 108–145 ppm was the main C-containing functional group in all biochars (45.0–80.3%), with an H_F of being 0.15. The aromatic C in biochars increased from 2.24% at 200 °C to 62.9% at 650 °C with H_T being 0.68 (Table 3). Therefore, the aromatic C was mainly controlled by the production temperature, agreeing with the recalcitrance shown above.

Similar dominant effect of production temperature compared to feedstock was observed for other C-containing functional groups. For example, the subdominant abundance of C was alkyl C (mainly CH_2 and CH_3 sp^3 carbons) at the chemical shift of 0–46 ppm accounted for 10.9–18.6% of the C-containing functional groups in biochar of different feedstock at production temperature of 500 °C (H_F = 0.15) and for 3.17–38.8% in biochar of different temperatures (H_T = 0.90). The 200 °C biochar retained properties comparable to the raw materials. For example, the C within 46–65 ppm and 65–90 ppm, representing methoxy and N alkyl C from OCH_3, C—N and complex aliphatic carbons, respectively, as well as O-alkyl C was in high proportions.

The FTIR spectra also indicate a range of superficial functional groups among different biochars (Fig. 3). The absorption peaks at 2916 cm^{-1} are assigned to saturated C—H stretching vibration (aliphatic C—H), and a wide absorption peak at 3200–3500 cm^{-1} is attributed to —OH stretching [21]. These peaks existed in all feedstock, but disappeared in biochar produced at temperature above 350 °C, as a result of dehydration of cellulosic and ligneous components (Fig. 3c and d). The dehydrogenation of methylene groups, which yielded increasingly condensed structures (R—CH_2—R → R=CH—R → R=C=R), controlled biochar recalcitrance (37). The peaks at 1465–1340 cm^{-1} are saturated C—H bending vibration and it is of great difference among biochars of feedstocks, while less difference among biochars produced at different temperatures. The —COO anti-symmetric stretching of amino acids (1574 and 1600 cm^{-1}) appeared in wood and crop waste biochars, which presented little change until the temperature rose to 650 °C. The intensity of C=O stretching of aromatic rings (1593 cm^{-1}) decreased with temperature rise and seemed similar in all feedstocks. Peaks at 874 and 1034 cm^{-1} were assigned to the bands of the out-of-plane bending for CO_3^{2-}, which exists more in biochars

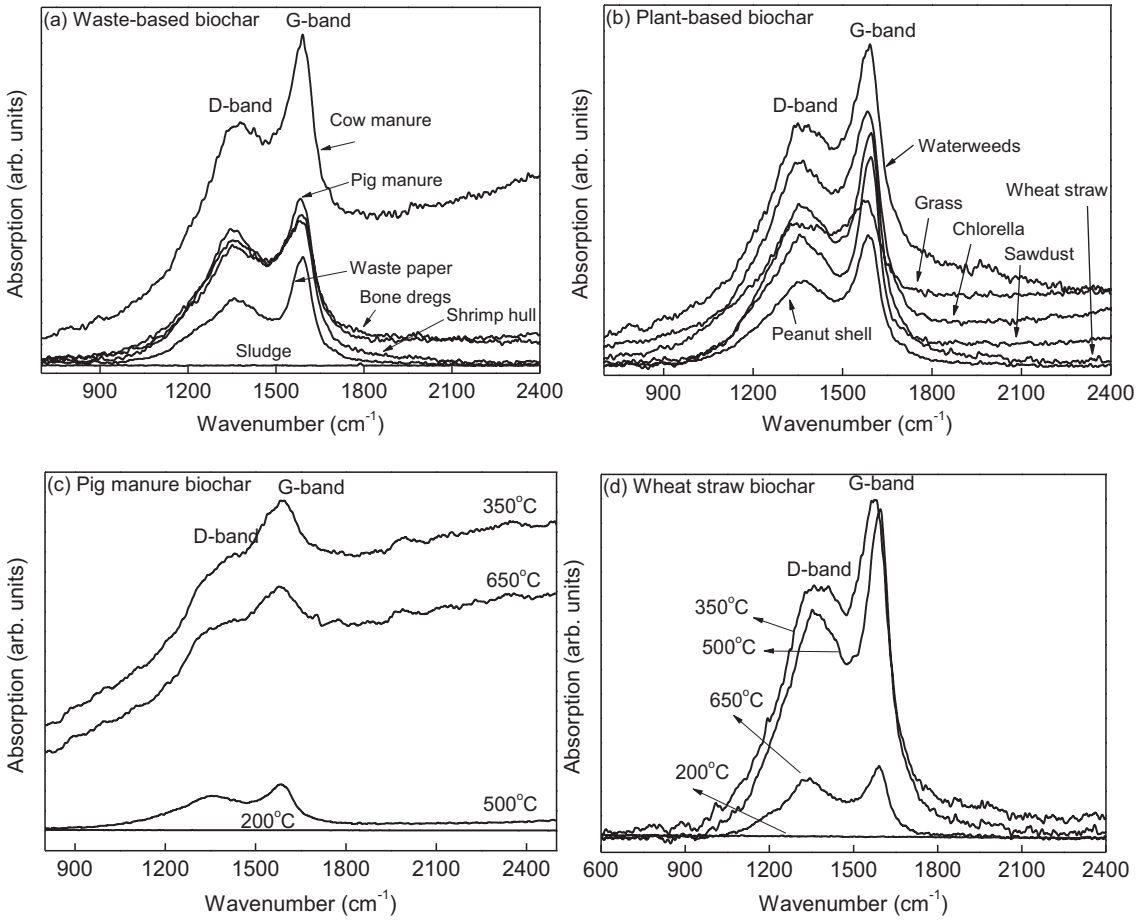

Fig. 4. Raman spectra of biochars derived from 12 feedstocks at 500 °C (a and b) and biochars produced from pig manure (c) and wheat straw at production temperature ranging 200–650 °C (d).

Table 3
Relative proportion (% of biochar-C) of chemical functional groups in biochars derived from 12 feedstocks at 500 °C and biochars produced from pig manure and wheat straw at 200–650 °C, determined by CP-MAS ^{13}C NMR.

Biochar feedstock	Temperature[a]	Chemical shift (ppm), δ								
		0–46	46–65	65–90	90–108	108–145	145–160	160–185	185–225	225–250
Cow manure	500 °C	10.87	–	–	3.59	61.4	7.68	4.79	6.48	6.58
Pig manure		11.7	2.9	16.0	4.20	45.0	2.80	18.6	0.40	–
Shrimp hull		12.7	1.9	2.50	6.00	75.0	4.10	–	–	1.90
Bone dregs		13.4	–	1.20	7.58	72.9	4.89	0.30	–	1.10
Wastewater sludge		18.6	1.5	5.10	5.90	63.4	5.30	–	0.70	1.90
Waste paper		13.7	–	0.20	2.49	75.0	5.28	–	–	5.18
Sawdust		12.4	–	1.00	2.29	78.3	2.89	–	–	5.08
Grass		11.0	0.00	0.00	2.50	80.3	2.79	0.30	–	4.29
Wheat straw		12.6	–	–	1.30	79.1	3.49	–	0.90	4.39
Peanut shell		12.5	0.80	–	1.60	79.6	3.90	–	–	3.90
Chlorella		13.4	0.60	1.30	3.70	77.3	2.80	–	–	3.90
Waterweeds		12.4	2.50	0.10	10.4	65.7	4.00	–	0.70	4.60
	H_F[b]	0.15	1.85	2.20	0.63	0.15	0.35	5.62	8.37	0.65
Pig manure	200 °C	38.8	20.6	27.8	5.37	2.79	0.60	7.56	–	–
	350 °C	38.3	5.74	11.3	6.82	34.7	3.80	7.98	–	–
	500 °C	11.7	2.9	16.0	4.20	45.0	2.80	18.6	0.40	–
	650 °C	3.17	–	1.29	7.14	57.6	3.17	1.78	11.5	14.7
	H_T[c]	0.80	1.28	0.78	0.23	0.67	0.54	0.78	5.51	4.44
Wheat straw	200 °C	3.77	13.3	66.9	14.0	1.69	0.89	–	–	–
	350 °C	33.7	4.59	0.80	3.59	49.4	7.98	0.10	–	0.40
	500 °C	12.6	–	–	1.30	79.1	3.49	–	0.90	4.39
	650 °C	5.47	1.00	3.18	6.17	68.2	4.78	3.68	4.28	3.28
	H_T	0.99	1.33	1.87	0.88	0.69	0.69	3.05	1.96	1.10

Note: The spectra were integrated in the chemical shift (ppm) resonance intervals of 0–46 ppm (alkyl C, mainly CH_2 and CH_3 sp^3 carbons), 46–65 ppm (methoxy and N alkyl C from OCH_3, C—N and complex aliphatic carbons), 65–90 ppm (O-alkyl C, such as alcohols and ethers), 90–108 ppm (anomeric carbons in carbohydrate-like structures), 108–145 ppm (aromatic and phenolic carbon), 145–160 ppm (oxygen aromatic carbon and olefinic sp^2 carbons), 160–185 ppm (carboxyl, amides and ester) and 185–225 ppm (carbonyls).

[a] Biochar production temperature.
[b] H_F, feedstock-depended heterogeneity.
[c] H_T, temperature-depended heterogeneity.

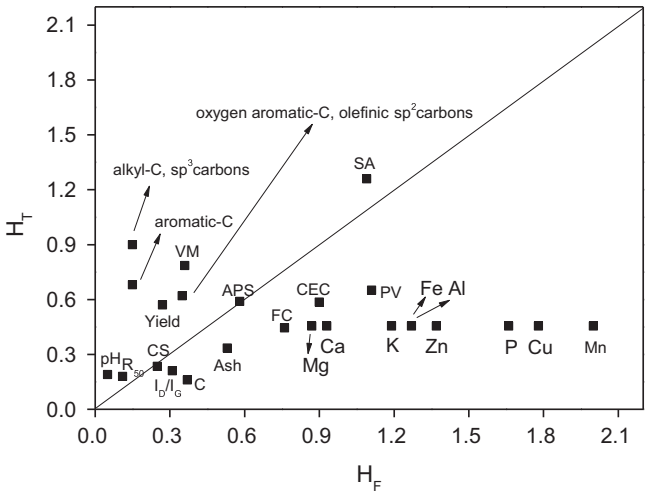

Fig. 5. Comparison of feedstock-depended heterogeneity (H_F) and temperature-depended heterogeneity (H_T) for different properties of biochar. See Table 1 for abbreviation.

of wastes and manures and less in plant-based biochars, and was less influenced by production temperature [38,39]. The NMR and FTIR results all showed the aromatization among different feedstocks and production temperature [40]. The recalcitrance and C sequestration have close relationship with carbon configuration, which perhaps determines the breakdown of C-bond and re-aggregation of C cluster under heat treatment [41].

Raman spectroscopy has been widely used to evaluate the microstructure of carbon materials, particularly the distribution and state of sp^2-bonded (aromatic) carbon [42], which is embedded in a disordered and amorphous matrix of both sp^3 and sp^2 carbon. The G-band centered at 1580 cm^{-1} arises from the in-plane vibrations of the sp^2-bonded crystallite carbon and has been observed for single crystal graphite, while another peak denoted as the "disorder" peak (or D-band) centered at 1357 cm^{-1} is typically observed in polycrystalline graphite. The D-band is attributed to in-plane vibrations of sp^2-bonded carbon within structural defects. For disordered carbon materials the ratio of the integrated intensities I_D/I_G is often reported to be inversely proportional to the lateral extension La of the graphene materials [43].

As shown in Fig. 4a and b, both G-band and D-band appeared in all 12 biochars with production temperature of 500 °C and had the similar I_D/I_G (0.804–1.51), with low H_F (0.31) (Table 1), implying that ratio of disordered or strongly distorted structure of turbostratic carbon to ordered graphite crystals was less determined by feedstocks than production temperature. For biochars produced at a range of production temperature, bands were found to develop at 350 °C, indicating the beginning of aromatization. The increase of I_D/I_G with temperature increasing from 350 °C to 650 °C was also not obvious (H_T < 0.36) since the temperature used in this study was in a relatively low range and their influence on biochar microstructure could be negligible.

4. Conclusions

This study quantitatively showed the extent to which feedstock and highest treatment temperature affect different biochar properties and yield. The results summarizing relationship between H_F and H_T for a range of properties in the biochar examined are shown in Fig. 5. The results clearly show that certain properties are predominantly controlled by production temperature, e.g., biochar yield, pH, recalcitrance and volatile matter, and therefore any applications of biochar requiring these properties would call for greater attention to the production temperature. Other properties are predominantly controlled by feedstock, e.g., biochar C content, CEC, fixed C, carbon sequestration capacity, mineral concentrations, and ash content, and therefore any applications of biochar requiring these properties would call for greater attention to the choice of feedstock.

Overall, the results of this study indicate that by appropriate combination of feedstock and production temperature it is possible to influence biochar properties to different degrees and therefore is should be possible to develop 'designed' biochar for specific environmental/agricultural applications.

Acknowledgements

This work was in part supported by the National Natural Science Foundation of China (No. 21077072, 21107070), Shanghai Pujiang Talent Project (11PJ1404600), and the University Innovation Project (AE1600004).

References

[1] T. Whitman, C.F. Nicholson, D. Torres, J. Lehmann, Climate change impact of biochar cook stoves in western Kenyan farm households: system dynamics model analysis, Environ. Sci. Technol. 45 (2011) 3687–3694.
[2] D. Matovic, Biochar as a viable carbon sequestration option: global and Canadian perspective, Energy 36 (2011) 2011–2016.
[3] K.G. Roberts, B.A. Gloy, S. Joseph, N.R. Scott, J. Lehmann, Life cycle assessment of biochar systems: estimating the energetic, economic, and climate change potential, Environ. Sci. Technol. 44 (2010) 827–833.
[4] X.D. Cao, L. Ma, B. Gao, W. Harris, Dairy-manure derived biochar effectively sorbs lead and atrazine, Environ. Sci. Technol. 43 (2009) 3285–3291.
[5] B.L. Chen, D.D. Zhou, L.Z. Zhu, Transitional adsorption and partition of nonpolar and polar aromatic contaminants by biochars of pine needles with different pyrolytic temperatures, Environ. Sci. Technol. 42 (2008) 5137–5143.
[6] H.L. Lu, W.H. Zhang, Y.X. Yang, X.F. Huang, S.Z. Wang, R.L. Qiu, Relative distribution of Pb^{2+} sorption mechanisms by sludge-derived biochar, Water Res. 46 (2012) 854–862.
[7] K.A. Spokas, K.B. Cantrell, J.M. Novak, D.W. Archer, J.A. Ippolito, Biochar: a synthesis of its agronomic impact beyond carbon sequestration, J. Environ. Qual. 41 (2012) 973–989.
[8] M.K. Hossain, V. Strezov, K.Y. Chan, P.F. Nelson, Agronomic properties of wastewater sludge biochar and bioavailability of metals in production of cherry tomato (*Lycopersicon esculentum*), Chemosphere 78 (2010) 1167–1171.
[9] A.R. Zimmerman, Abiotic and microbial oxidation of laboratory-produced lack carbon (Biochar), Environ. Sci. Technol. 44 (2010) 1295–1301.
[10] E.R. Graber, Y.M. Harel, M. Kolton, E. Cytryn, A. Silber, D.R. David, L. Tsechansky, M. Borenshtein, Y. Elad, Biochar impact on development and productivity of pepper and tomato grown in fertigated soilless media, Plant Soil 337 (2010) 481–496.
[11] M.I. Bird, C.M. Wurster, P.H. de Paula Silva, A.M. Bass, R. de Nys, Algal biochar–production and properties, Bioresour. Technol. 102 (2010) 1886–1891.
[12] J.M. Novak, W.J. Busscher, Evaluation of designer biochars to ameliorate select chemical and physical characteristics of degraded soils, in: AIChE Annual Meeting, Nashville, 2009.
[13] A. Enders, K. Hanley, T. Whitman, S. Joseph, J. Lehmann, Characterization of biochars to evaluate recalcitrance and agronomic performance, Bioresour. Technol. 114 (2012) 644–653.
[14] M.K. Hossain, V. Strezov, K.Y. Chan, A. Ziolkowski, P.F. Nelson, Influence of pyrolysis temperature on production and nutrient properties of wastewater sludge biochar, J. Environ. Manage. 92 (2011) 223–228.
[15] J.H. Yuan, R.K. Xu, H. Zhang, The forms of alkalis in the biochar produced from crop residues at different temperatures, Bioresour. Technol. 102 (2011) 3488–3497.
[16] A. Mukherjee, A.R. Zimmerman, W. Harris, Surface chemistry variations among a series of laboratory-produced biochars, Geoderma 163 (2011) 247–255.
[17] S. Kloss, F. Zehetner, A. Dellantonio, R. Hamid, F. Ottner, V. Liedtke, M. Schwanninger, M.H. Gerzabek, G. Soja, Characterization of slow pyrolysis biochars: effects of feedstocks and pyrolysis temperature on biochar properties, J. Environ. Qual. 41 (2012) 990–1000.
[18] K.B. Cantrell, P.G. Hunt, M. Uchimiya, J.M. Novak, K.S. Ro, Impact of pyrolysis temperature and manure source on physicochemical characteristics of biochar, Bioresour. Technol. 107 (2012) 419–428.
[19] R.C. Pereira, J. Kaal, M.C. Arbestain, R.P. Lorenzo, W. Aitkenhead, M. Hedley, F. Macías, J. Hindmarsh, J.A. Maciá-Agulló, Contribution to characterisation of biochar to estimate the labile fraction of carbon, Org. Geochem. 42 (2011) 1331–1342.
[20] J.A. Ippolito, D.A. Laird, W.J. Busscher, Environmental benefits of biochar, J. Environ. Qual. 41 (2012) 967–972.

[21] X.D. Cao, W. Harris, Properties of dairy-manure-derived biochar pertinent to its potential use in remediation, Bioresour. Technol. 101 (2010) 5222–5228.
[22] Standard test method for ash in the analysis sample of coal and coke from coal. Designation: D3174-11. ASTM Committee, 2011.
[23] Standard test method for volatile matter in the analysis sample of coal and coke. Designation: D3175-11. ASTM Committee, 2007.
[24] Standard practice for proximate analysis of coal and coke. Designation: D3172-07a. ASTM Committee, 2007.
[25] U.S. Environmental Protection Agency (USEPA), Test Methods for Evaluating Solid Waste, Laboratory Manual Physical/Chemical Methods, U.S. Gov. Print Office, Washington, DC, 1986.
[26] J.W. Lee, M. Kidder, B.R. Evans, S. Paik, A.C. Buchanan, C.T. Garten, R.C. Brown, Characterization of biochars produced from cornstovers for soil amendment, Environ. Sci. Technol. 44 (2010) 7970–7974.
[27] O.R. Harvey, L.J. Kuo, A.R. Zimmerman, P. Louchouarn, J.E. Amonette, B.E. Herbert, An index-based approach to assessing recalcitrance and soil carbon sequestration potential of engineered black carbons (Biochars), Environ. Sci. Technol. 46 (2012) 1415–1421.
[28] K. Crombie, M. Ondřej, S.P. Saran, B. Peter, C. Andrew, The effect of pyrolysis conditions on biochar stability as determined by three methods, GCB Bioenergy 5 (2013) 122–131.
[29] D.A. Laird, P. Fleming, D.D. Davis, R. Horton, B. Wang, D.L. Karlen, Impact of biochar amendments on the quality of a typical Midwestern agricultural soil, Geoderma 158 (2010) 443–449.
[30] C.J. Atkinson, J.D. Fitzgerald, N.A. Hipps, Potential mechanisms for achieving agricultural benefits from biochar application to temperate soils: a review, Plant Soil 337 (2010) 1–18.
[31] K.Y. Chan, L. van Zwieten, I. Meszaros, A. Downie, S. Joseph, Agronomic values of greenwaste biochar as a soil amendment, Austra, J. Soil Res. 45 (2007) 629–634.
[32] K.A. Spokas, W.C. Koskinen, J.M. Baker, D.C. Reicosky, Impacts of woodchip biochar additions on greenhouse gas production and sorption/degradation of two herbicides in a Minnesota soil, Chemosphere 77 (2009) 574–581.
[33] C.H. Cheng, J. Lehmann, J.E. Thies, S.D. Burton, M.H. Engelhard, Oxidation of black carbon by biotic and abiotic processes, Org. Geochem. 37 (2006) 1477–1488.
[34] N. Worasuwannarak, T. Sonobe, W. Tanthapanichakoon, Pyrolysis behaviors of rice straw, rice husk, and corncob by TG-MS technique, J. Anal. Appl. Pyrolysis 78 (2007) 265–271.
[35] O. Mašek, P. Brownsort, A. Cross, S. Sohi, Influence of production conditions on the yield and environmental stability of biochar, Fuel 103 (2013) 151–155, 2011.
[36] K. Jindo, K. Suto, K. Matsumoto, C. García, T. Sonoki, M.A. Sanchez-Monedero, Chemical and biochemical characterisation of biochar-blended composts prepared from poultry manure, Bioresour. Technol. 110 (2012) 396–404.
[37] R.O. Harvey, B.E. Herbert, L.J. Kuo, P. Louchouarn, Generalized two-dimensional perturbation correlation infrared spectroscopy reveals mechanisms for the development of surface charge and recalcitrance in plant-derived biochars, Environ. Sci. Technol. 46 (2012) 10641–10650.
[38] L. Beesley, E. Moreno-Jiménez, J.L. Gomez-Eyles, Effects of biochar and greenwaste compost amendments on mobility, bioavailability and toxicity of inorganic and organic contaminants in a multi-element polluted soil, Environ. Pollut. 158 (2010) 2282–2287.
[39] B. Singh, B.P. Singh, A.L. Cowie, Characterisation and evaluation of biochars for their application as a soil amendment, Austra, J. Soil Res. 48 (2010) 516–525.
[40] M. Keiluweit, P.S. Nico, M.G. Johnson, M. Kleber, Dynamic molecular structure of plant biomass-derived black carbon (Biochar), Environ. Sci. Technol. 44 (2010) 1247–1253.
[41] B.T. Nguyen, J. Lehmann, W.C. Hockaday, S. Joseph, C.A. Masiello, Temperature sensitivity of black carbon decomposition and oxidation, Environ. Sci. Technol. 44 (2010) 3324–3331.
[42] Y.R. Rhim, D.J. Zhang, D.H. Fairbrother, K.A. Wepasnick, K.J. Livi, R.J. Bodnar, D.C. Nagle, Changes in electrical and microstructural properties of microcrystalline cellulose as function of carbonization temperature, Carbon 48 (2010) 1012–1024.
[43] O. Paris, C. Zollfrank, G.A. Zickler, Decomposition and carbonisation of wood biopolymers-a microstructural study of softwood pyrolysis, Carbon 43 (2005) 53–66.